Spectroscopic Features of Quantum Many-Body Scar States

Wenjie Wei[1] and Long Zhang[1,2*]

[1]*Kavli Institute for Theoretical Sciences and CAS Center for Excellence in Topological Quantum Computation, University of Chinese Academy of Sciences, Beijing 100190, China*
[2]*Hefei National Laboratory, Hefei 230088, China*

(Received 3 October 2024; accepted manuscript online 31 January 2025)

We studied the dynamic correlations of non-integrable systems with quantum many-body scar (QMBS) states generated by a ladder operator. The ladder operator's spectral function has an exact δ-function peak induced by the QMBS states. As a concrete example, we show that in the one-dimensional (1D) spin-1 Affleck–Kennedy–Lieb–Tasaki model, the spectral function of two-magnon excitations exhibits a characteristic bowtie shape composed of a δ-function resonance peak at momentum $k = \pi$ and a continuum spectrum elsewhere. The two-magnon excitations can be observed via resonant inelastic X-ray scattering spectroscopy on quasi-1D nickelates and other spin-1 antiferromagnetic materials. Therefore, the findings of this study pave the way for detecting (approximate) QMBS states in realistic materials.

DOI: 10.1088/0256-307X/42/2/020502 CSTR: 32039.14.0256-307X.42.2.020502

Introduction. Quantum many-body scar (QMBS) states are a typical class of nonthermalizing eigenstates in certain non-integrable quantum systems.[1–12] For a generic non-integrable quantum many-body system, it has been postulated that the physical observables of highly excited eigenstates vary smoothly with energy up to small fluctuations that vanish in the thermodynamic limit. Therefore, an eigenstate is physically indistinguishable from the microcanonical ensemble. The eigenstate thermalization hypothesis (ETH) lays the conceptual foundation of quantum statistical physics.[13–17] However, certain non-integrable quantum systems have QMBS eigenstates whose physical properties strongly deviate from the adjacent eigenstates in the energy spectrum and the microcanonical ensemble. Particularly, their entanglement entropy exhibits sub-volume-law scaling instead of the volume-law scaling expected for generic eigenstates that obey the ETH.[1,2,4] Therefore, QMBS states violate the ETH and have recently attracted increased research interest.

A variety of QMBS states can be constructed using spectrum-generating algebra (SGA) formalism.[3,18] Starting from a reference eigenstate $|G\rangle$ with energy ϵ_{G}, a tower of QMBS states $|S_n\rangle$ ($n \in \mathbb{N}$) is obtained by iteratively applying a ladder operator $Q^\dagger$ to $|G\rangle$, $|S_n\rangle = (Q^\dagger)^n|G\rangle$. Here, ladder operator $Q^\dagger$ is the summation of the local (finite-range) operators and satisfies $[H, Q^\dagger]|S_n\rangle = \xi Q^\dagger|S_n\rangle$ ($n \in \mathbb{N}$). Therefore, these $|S_n\rangle$ form an equally spaced tower of QMBS states $H|S_n\rangle = (\epsilon_G + n\xi)|S_n\rangle$. The SGA formalism applies to the one-dimensional (1D) Affleck–Kennedy–Lieb–Tasaki (AKLT) model,[3] generalized spin-1 XY model,[19] and generalized Hubbard model,[20] among others. This has been generalized to the quasi-symmetry group formalism of QMBS states.[21]

The QMBS states tower leads to the constant revival of physical quantities in real-time evolution if the initial state has a substantial overlap with the QMBS states,[1,2] whereas the physical quantities of a generic initial state obeying the ETH quickly relax to the thermal equilibrium state. Such anomalous long-term revival phenomena owing to QMBS states have been observed in quantum simulation experiments using Rydberg atom arrays and other platforms.[22–25]

In this study, we investigated the dynamic correlations of quantum many-body systems with scar states. We demonstrate that the spectral function of the SGA ladder operator has an exact δ-function peak owing to the QMBS states. Particularly, we found that in the 1D AKLT model, the spectral function of two-magnon excitations exhibits a characteristic bow tie shape consisting of a δ-function resonance peak at momentum $k = \pi$ and continuum spectra at other generic momenta. The resonance peak persisted, but broadened when the Hamiltonian was slightly deformed away from the AKLT model. We propose that the two-magnon spectrum can be observed via resonant inelastic X-ray scattering (RIXS) experiments on quasi-1D nickelates and other spin-1 antiferromagnetic (AF) materials, thereby providing spectroscopic evidence of (approximate) QMBS states in realistic materials.

SGA and Spectral Function in the AKLT Model. The 1D AKLT model is a spin-1 AF Heisenberg model deformed by a biquadratic term[26,27]

$$H = \sum_{l=1}^{L} P_{l,l+1} = \sum_{l=1}^{L} \left(\frac{1}{3} + \frac{1}{2}\boldsymbol{S}_l \cdot \boldsymbol{S}_{l+1} + \frac{1}{6}(\boldsymbol{S}_l \cdot \boldsymbol{S}_{l+1})^2\right), \quad (1)$$

where $P_{l,l+1}$ is the projection operator in the total spin-2 subspace of sites l and $l+1$. The ground state of the AKLT

*Corresponding author. Email: longzhang@ucas.ac.cn
© 2025 Chinese Physical Society and IOP Publishing Ltd. All rights, including for text and data mining, AI training, and similar technologies, are reserved.

model with periodic boundary conditions is the unique common eigenstate of all $P_{l,l+1}$ with eigenvalue 0. This can be represented by the following matrix product state (MPS):[28–30]

$$|G\rangle = \sum_{\{s_l\}} \mathrm{Tr}\Big(\prod_{l=1}^{L} M^{[s_l]}\Big)|s_1 s_2 \cdots s_L\rangle, \tag{2}$$

where $|s_l\rangle$ ($s_l = 0, \pm 1$) are the eigenstates of S_l^z with eigenvalue s_l. The matrices are expressed as follows:

$$M^{[1]} = \begin{pmatrix} 0 & \sqrt{2} \\ 0 & 0 \end{pmatrix}, \; M^{[0]} = \begin{pmatrix} -1 & 0 \\ 0 & 1 \end{pmatrix}, \\ M^{[-1]} = \begin{pmatrix} 0 & 0 \\ -\sqrt{2} & 0 \end{pmatrix}. \tag{3}$$

The ground state is a short-range correlated disordered state with a spin correlation length of $\xi = 1/\ln 3$.[26,27] The AKLT model has a finite excitation gap,[26,27] which agrees with the Haldane conjecture for integer-spin AF Heisenberg chains.[31,32] Additionally, the AKLT model is a prominent example of symmetry-protected topological order with degenerate edge states under open boundary conditions.[33,34]

A QMBS states tower in the AKLT model can be constructed by applying the following ladder operator to the ground state,[3]

$$Q_\pi^\dagger = \frac{1}{\sqrt{L}} \sum_{l=1}^{L} (-1)^l (S_l^+)^2, \tag{4}$$

$|S_n\rangle = (Q_\pi^\dagger)^n |G\rangle$ ($0 \le n \le L/2$). These states satisfy $[H, Q_\pi^\dagger]|S_n\rangle = 2Q_\pi^\dagger |S_n\rangle$. Therefore, the $|S_n\rangle$ form a eigenstates tower with energy $\epsilon_n = 2n$. These states can also be efficiently represented via MPS with virtual bond dimensions bounded by L. Therefore, their entanglement entropy exhibits sub-volume-law scaling,[4] which is a hallmark of QMBS states. Furthermore, $Q_\pi = (Q_\pi^\dagger)^\dagger$ generates another QMBS states tower $|\tilde{S}_n\rangle = Q_\pi^n |G\rangle$ with energy $\tilde{\epsilon}_n = 2n$, as Q_π and $Q_\pi^\dagger$ are related by the spin rotation symmetry transformation $R_x(\pi) = \otimes_l e^{i\pi S_l^x}$, $Q_\pi = R_x(\pi) Q_\pi^\dagger R_x(\pi)^\dagger$.

Moreover, operator $Q_k^\dagger$ satisfies

$$Q_k^\dagger = \frac{1}{\sqrt{L}} \sum_{l=1}^{L} e^{ilk} (S_l^+)^2 = \frac{1}{\sqrt{L}} \sum_q S_q^+ S_{k-q}^+, \tag{5}$$

where $S_q^+ = L^{-1/2} \sum_{l=1}^{L} e^{iql} S_l^+$. $Q_k^\dagger$ creates a two-magnon excitation with a total momentum k, therefore, QMBS state $|S_1\rangle = Q_\pi^\dagger |G\rangle$ is the exact bound state of the two-magnon excitations. However, $Q_k^\dagger |G\rangle$ ($k \neq \pi$) is generally not an exact eigenstate.

In this study, we considered the retarded Green's function of two-magnon excitations at zero temperature:

$$G(\omega, k) = -i \int_0^\infty dt \, e^{i(\omega + i0^+)t} \langle G|[Q_k(t), Q_k^\dagger(0)]|G\rangle. \tag{6}$$

The spectral function $A(\omega, k) = -\frac{1}{\pi} \mathrm{Im} G(\omega, k)$ can be expressed in the Lehmann's spectral representation as follows:

$$A(\omega, k) = \sum_\alpha |\langle \alpha | Q_k^\dagger | G\rangle|^2 \delta(\omega - \epsilon_\alpha) \\ - \sum_\alpha |\langle \alpha | Q_k | G\rangle|^2 \delta(\omega + \epsilon_\alpha), \tag{7}$$

where the summation is performed over the complete eigenstate basis $|\alpha\rangle$ with excitation energy $\epsilon_\alpha \ge 0$. Furthermore, we have $A(\omega, k) = -A(-\omega, k)$ because $Q_k^\dagger$ and Q_k are related by the symmetry transformation composed of spin rotation $R_x(\pi)$ and space inversion $\mathcal{I}$. For the AKLT model, the spectral function at momentum $k = \pi$ has δ-function resonance peaks due to QMBS states $|S_1\rangle = Q_\pi^\dagger |G\rangle$ and $|\tilde{S}_1\rangle = Q_\pi |G\rangle$, $A(\omega, k = \pi) \propto \delta(\omega - 2) - \delta(\omega + 2)$. For $k \neq \pi$, $A(\omega, k)$ exhibits a continuum spectrum, thus forming a characteristic bow tie shape, as shown in the numerical results discussed later.

For the AKLT model, we have the following sum rule:

$$\int_0^\infty \mathrm{d}\omega \, A(\omega, k) = \frac{4}{3}, \quad \forall k. \tag{8}$$

This is proven by the fact that the integral is given by the static structure factor of the two-magnon operator at the ground state,

$$\langle G | Q_k Q_k^\dagger | G\rangle = \frac{1}{L} \sum_{ll'} e^{ik(l'-l)} \langle G | (S_l^-)^2 (S_{l'}^+)^2 | G\rangle. \tag{9}$$

The correlation function of the two-spin-flip operator satisfies the following:

$$\langle G | (S_l^-)^2 (S_{l'}^+)^2 | G\rangle = \frac{4}{3} \delta_{ll'}, \quad L \to \infty. \tag{10}$$

The vanishing correlation function for $l \neq l'$ is derived from the strictly diluted AF order of the AKLT ground state.[26,27,35]

Numerical Results. The two-magnon spectral functions of the AKLT model and deformed Hamiltonian in Eq. (16) were calculated using the MPS-based density matrix renormalization group (DMRG)[29,30,36–38] and the KPM.[39] The ground state $|G\rangle$ under the periodic boundary condition was obtained using the DMRG algorithm and was represented by an MPS. In the KPM, the Hamiltonian is first rescaled such that all eigenvalues are bounded in the interval $[-1, 1]$; then, its spectral function $A(\omega, k)$ for $\omega > 0$ is approximated by a truncated series:[39]

$$A(\omega, k) = \frac{1}{\pi \sqrt{1 - \omega^2}} \Big(g_0 \mu_0 + 2 \sum_{n=1}^{N-1} g_n \mu_n T_n(\omega) \Big) \tag{11}$$

of Chebyshev polynomials of the first kind, $T_n(\omega) = \cos(n \arccos \omega)$, in which the truncation order N is sufficiently large to guarantee convergence of the series. The expansion coefficients are expressed as

$$\mu_n = \langle G | Q_k T_n(H) Q_k^\dagger | G\rangle \equiv \langle \alpha_0 | \alpha_n \rangle, \tag{12}$$

in which $|\alpha_n\rangle = T_n(H) Q_k^\dagger |G\rangle$ are calculated by applying $Q_k^\dagger$ and H (represented by matrix-product operators) to $|G\rangle$ according to the iteration relation, $|\alpha_0\rangle = Q_k^\dagger |G\rangle$, $|\alpha_1\rangle = H|\alpha_0\rangle$, and $|\alpha_{n+1}\rangle = 2H|\alpha_n\rangle - |\alpha_{n-1}\rangle$ ($n \ge 1$). In Eq. (11), Lorentz kernel factors $g_n = \sinh(\lambda(1 - n/N))/\sinh\lambda$ are introduced to improve the behavior of the truncated series. This is equivalent to convolving the

spectral function with the Lorentz line-shape function with width $\eta = \lambda/N$,[39] therefore, it effectively mimics the finite resolution of the experimental apparatus. Subsequently, the frequency in the spectral function was rescaled back to the energy range of the original Hamiltonian.

The two-magnon spectral function of the AKLT model was calculated using the KPM, as shown in Fig. 1. A prominent feature is the resonance peak at $k = \pi$. As shown in Figs. 1(b)–1(g), the sharpness of this resonance peak is limited only by the Lorentz broadening width; therefore, it is consistent with the δ-function peak induced by the QMBS states, as proved previously. By contrast, the spectral function at $k \neq \pi$ approaches a continuum in the thermodynamic limit, indicating that two-magnon excitations do not form coherent quasiparticles. Therefore, the spectral function $A(\omega, k)$ has a characteristic bow tie shape composed of a δ-function resonance peak induced by the QMBS states at $k = \pi$ and a continuum spectrum elsewhere.

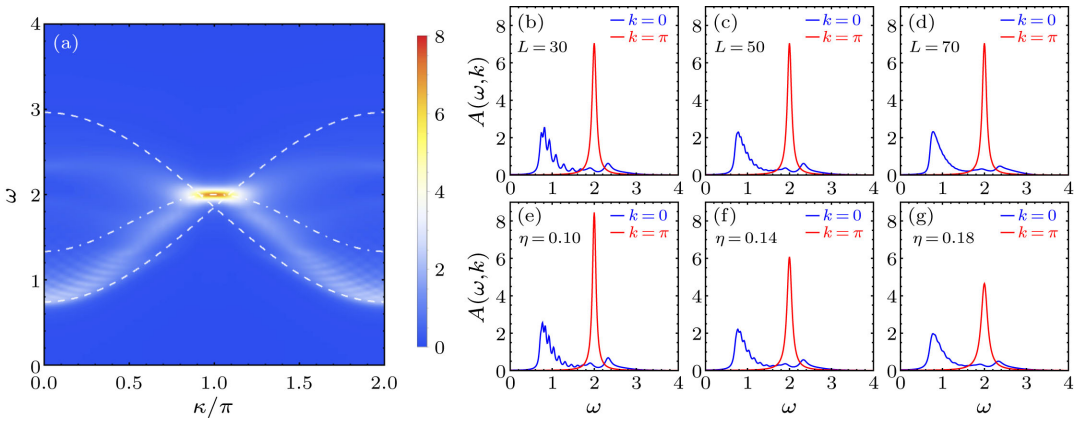

Fig. 1. (a) Two-magnon spectral function of the AKLT model at the ground state. The dot-dashed curve represents the average energy ε_k obtained using Eq. (13). The dashed curves represent the approximate upper and lower edges in Eq. (15) obtained with the single-mode approximation of one-magnon excitations. The numerical results are obtained on a lattice with $L = 40$ and periodic boundary conditions. The order of the kernel polynomial method (KPM) truncated series is $N = 1000$. The effective Lorentz broadening width is $\eta = 0.12$. (b)–(d) $A(\omega, k)$ comparison at $k = 0$ and π for different lattice sizes $L = 30$, 50, and 70 with the same Lorentz broadening width $\eta = 0.12$. The sharp resonance peak at $k = \pi$ barely changes, while the discrete peaks in $A(\omega, k)$ at $k = 0$ merge into a continuum spectrum in the thermodynamic limit. (e)–(g) $A(\omega, k)$ comparison at $k = 0$ and π with different Lorentz broadening widths $\eta = 0.10$, 0.14, and 0.18 for the same lattice size $L = 40$. The sharpness of the peak at $k = \pi$ is only limited by the Lorentz broadening, which is consistent with a δ-function peak induced by the QMBS states.

The average energy of the two-magnon excitations $Q_k^\dagger|G\rangle$ can be calculated analytically using the method described in Ref. [27]. The result is given by

$$\varepsilon_k = \frac{\langle G|Q_k H Q_k^\dagger|G\rangle}{\langle G|Q_k Q_k^\dagger|G\rangle} = \frac{1}{3}(5 - \cos k), \tag{13}$$

as shown in Fig. 1(a). The energy of a two-magnon excitation with total momentum k can also be approximated by summing the energy of two one-magnon excitations, $E_k = \xi_q + \xi_{k-q}$, in which the one-magnon energy ξ_q is estimated using single-mode approximation:[40]

$$\xi_q \simeq \frac{\langle G|S_{-q}^- H S_q^+|G\rangle}{\langle G|S_{-q}^- S_q^+|G\rangle} = \frac{5}{27}(5 + 3\cos q). \tag{14}$$

Thus, we have $E_k \simeq \frac{10}{27}(5 + 3\cos(k/2)\cos(k/2 - q))$, which is bounded by

$$\frac{10}{27}(5 - 3|\cos(k/2)|) \lesssim E_k \lesssim \frac{10}{27}(5 + 3|\cos(k/2)|). \tag{15}$$

This is a good approximation of the upper and lower edges of the two-magnon spectrum, as shown in Fig. 1(a).

Then, we consider the following spin-1 bilinear-biquadratic Hamiltonian:[41]

$$H = \sum_{l=1}^{L}\left(\frac{1}{3} + \frac{1}{2}\boldsymbol{S}_l \cdot \boldsymbol{S}_{l+1} + \frac{\alpha}{6}(\boldsymbol{S}_l \cdot \boldsymbol{S}_{l+1})^2\right), \tag{16}$$

which is a deformation of the AKLT model and is relevant for realistic quasi-1D AF materials, such as $LiVGe_2O_6$.[42,43] The two-magnon spectral functions $A(\omega, k)$ for $\alpha = 0.5$ and 1.5 are shown in Fig. 2. The exact SGA relation breaks down in the deformed Hamiltonian, and $Q_\pi^\dagger|G\rangle$ is not an exact eigenstate. Therefore, the resonance peak at $k = \pi$ is no longer a δ-function. However, the spectral function maintains the overall bow tie shape with a sharp resonance peak (although with finite width) at $k = \pi$ and a broad continuum elsewhere. This is reminiscent of the atypical eigenstates with low entanglement entropy observed in the deformed Hamiltonian in Ref. [4].

Proposed RIXS Experiments. We propose that the characteristic bow tie shape of the two-magnon spectral function induced by the QMBS states can be detected via RIXS spectroscopy of quasi-1D spin-1 AF nickelates such as $CsNiCl_3$ and $Ni(C_2H_8N_2)_2NO_2ClO_4$ (NENP). The one-magnon excitations of these materials were observed via inelastic neutron scattering spectroscopy, exhibiting an energy gap of spin excitations,[44–47] which supports the Haldane gap of spin-1 AF chains. In the RIXS of spin-1 magnetic materials, the differential scattering cross-section is given by the spectral function of an effective scattering operator $R_j^{\varepsilon_i\varepsilon_o}$.[48] When the polarization of the incoming and outgoing X-ray beams are given by

$\varepsilon_i = \varepsilon_o^* = (1, i)/\sqrt{2}$, i.e., they are left and right circularly polarized, respectively, the spin transfer in the scattering process is $\Delta S = +2$, then the scattering operator at site j is given by $R_j^{\varepsilon_i \varepsilon_o} = \sigma^{(0)} + \sigma^{(2)}(S_j^+)^2$, where $\sigma^{(0)}$ and $\sigma^{(2)}$ are constant factors.[48] Therefore, RIXS precisely measures the two-magnon spectral function $A(\omega, k)$ of spin-1 magnetic materials and can detect the characteristic bow tie shape induced by QMBS states in quasi-1D AF materials.

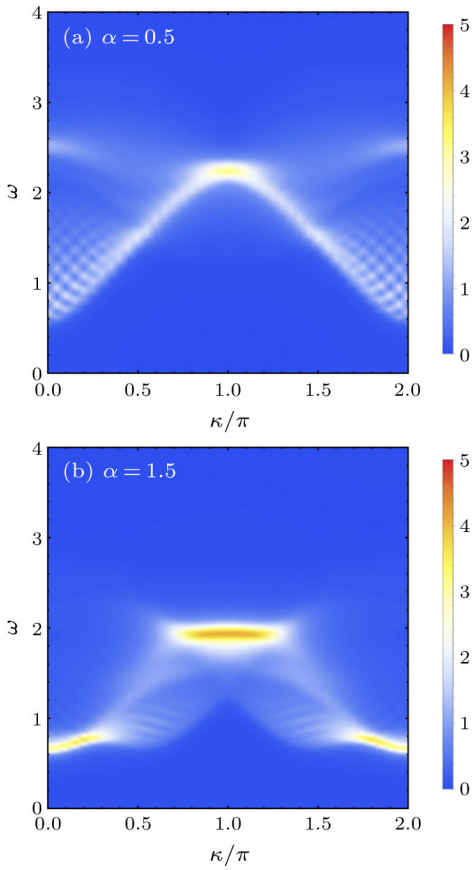

Fig. 2. Two-magnon spectral function $A(\omega, k)$ of the deformed Hamiltonian in Eq. (16) with (a) $\alpha = 0.5$ and (b) 1.5. The lattice size is $L = 40$. The order of the KPM truncated series is $N = 1000$. The effective Lorentz broadening width is $\eta = 0.22$.

Summary. We demonstrated that the QMBS states constructed with the SGA formalism produce a δ-function resonance peak in the spectral function of the SGA ladder operator. As a concrete example, we show that the two-magnon spectral function in the AKLT model exhibits a characteristic bow tie shape composed of a resonance peak at $k = \pi$ induced by the QMBS states and a continuum spectrum elsewhere. This overall bow tie shape persists in the deformed Hamiltonian with a broadened resonance peak. We propose that a two-magnon spectral function can be observed in RIXS experiments on quasi-1D nickelates and other spin-1 AF materials, thereby providing spectroscopic evidence for (approximate) QMBS states in realistic materials. Our results for the resonance peak in the spectral function also apply to other QMBS systems generated with the SGA formalism, for example, spin-1 generalized XY models in higher dimensions. Therefore, similar spectroscopic features are expected for these systems.

Added note. Upon completion of this work, we became aware of a recent work[49] in which the spectral function of QMBS systems was studied from the perspective of the quasi-symmetry group and quasi-Nambu-Goldstone mode.

Acknowledgements. L.Z. is grateful to Xue-Rong Liu and Xingye Lu for helpful discussions. Part of the numerical simulations were performed using the ITensor package.[50] This work was supported by the National Natural Science Foundation of China (Grant No. 12174387), the Chinese Academy of Sciences (Grant Nos. YSBR-057 and JZHKYPT-2021-08), and the Innovative Program for Quantum Science and Technology (Grant No. 2021ZD0302600).

References

[1] Turner C J, Michailidis A A, Abanin D A, Serbyn M, and Papić Z 2018 *Nat. Phys.* **14** 745
[2] Turner C J, Michailidis A A, Abanin D A, Serbyn M, and Papić Z 2018 *Phys. Rev. B* **98** 155134
[3] Moudgalya S, Rachel S, Bernevig B A, and Regnault N 2018 *Phys. Rev. B* **98** 235155
[4] Moudgalya S, Regnault N, and Bernevig B A 2018 *Phys. Rev. B* **98** 235156
[5] Ho W W, Choi S, Pichler H, and Lukin M D 2019 *Phys. Rev. Lett.* **122** 040603
[6] Khemani V, Laumann C R, and Chandran A 2019 *Phys. Rev. B* **99** 161101
[7] Lin C J and Motrunich O I 2019 *Phys. Rev. Lett.* **122** 173401
[8] Choi S, Turner C J, Pichler H, Ho W W, Michailidis A A, Papć Z, Serbyn M, Lukin M D, and Abanin D A 2019 *Phys. Rev. Lett.* **122** 220603
[9] Serbyn M, Abanin D A, and Papić Z 2021 *Nat. Phys.* **17** 675
[10] Papić Z 2022 *Entanglement Spin Chain* (Springer, Cham, Switzerland) p. 341
[11] Moudgalya S, Bernevig B A, and Regnault N 2022 *Reports Prog. Phys.* **85** 086501
[12] Chandran A, Iadecola T, Khemani V, and Moessner R 2023 *Annu. Rev. Condens. Matter Phys.* **14** 443
[13] Deutsch J M 1991 *Phys. Rev. A* **43** 2046
[14] Srednicki M 1994 *Phys. Rev. E* **50** 888
[15] Rigol M, Dunjko V, and Olshanii M 2008 *Nature* **452** 854
[16] D'Alessio L, Kafri Y, Polkovnikov A, and Rigol M 2016 *Adv. Phys.* **65** 239
[17] Deutsch J M 2018 *Reports Prog. Phys.* **81** 082001
[18] Mark D K, Lin C J, and Motrunich O I 2020 *Phys. Rev. B* **101** 195131
[19] Schecter M and Iadecola T 2019 *Phys. Rev. Lett.* **123** 147201
[20] Mark D K and Motrunich O I 2020 *Phys. Rev. B* **102** 075132
[21] Ren J, Liang C, and Fang C 2021 *Phys. Rev. Lett.* **126** 120604
[22] Bernien H, Schwartz S, Keesling A, Levine H, Omran A, Pichler H, Choi S, Zibrov A S, Endres M, Greiner M, Vuletić V, and Lukin M D 2017 *Nature* **551** 579
[23] Bluvstein D, Omran A, Levine H, Keesling A, Semeghini G, Ebadi S, Wang T T, Michailidis A A, Maskara N, Ho W W, Choi S, Serbyn M, Greiner M, Vuletić V, and Lukin M D 2021 *Science* **371** 1355
[24] Su G X, Sun H, Hudomal A, Desaules J Y, Zhou Z Y, Yang B, Halimeh J C, Yuan Z S, Papić Z, and Pan J W 2023 *Phys. Rev. Res.* **5** 023010

[25] Liang X, Yue Z, Chao Y X, Hua Z X, Lin Y, Tey M K, and You L 2024 arXiv:2410.16174
[26] Affleck I, Kennedy T, Lieb E H, and Tasaki H 1987 *Phys. Rev. Lett.* **59** 799
[27] Affleck I, Kennedy T, Lieb E H, and Tasaki H 1988 *Commun. Math. Phys.* **115** 477
[28] Klümper A, Schadschneider A, and Zittartz J 1993 *Europhys. Lett.* **24** 293
[29] Schollwöck U 2011 *Ann. Phys.* **326** 96
[30] Orús R 2014 *Ann. Phys.* **349** 117
[31] Haldane F D M 1983 *Phys. Lett. A* **93** 464
[32] Haldane F D M 1983 *Phys. Rev. Lett.* **50** 1153
[33] Gu Z C and Wen X G 2009 *Phys. Rev. B* **80** 155131
[34] Pollmann F, Turner A M, Berg E, and Oshikawa M 2010 *Phys. Rev. B* **81** 064439
[35] den Nijs M and Rommelse K 1989 *Phys. Rev. B* **40** 4709
[36] White S R 1992 *Phys. Rev. Lett.* **69** 2863
[37] White S R 1993 *Phys. Rev. B* **48** 10345
[38] Schollwöck U 2005 *Rev. Mod. Phys.* **77** 259
[39] Weiße A, Wellein G, Alvermann A, and Fehske H 2006 *Rev. Mod. Phys.* **78** 275
[40] Arovas D P 1989 *Phys. Lett. A* **137** 431
[41] Bursill R J, Xiang T, and Gehring G A 1995 *J. Phys. A. Math. Gen.* **28** 2109
[42] Millet P, Mila F, Zhang F C, Mambrini M, Van Oosten A B, Pashchenko V A, Sulpice A, and Stepanov A 1999 *Phys. Rev. Lett.* **83** 4176
[43] Lou J, Xiang T, and Su Z 2000 *Phys. Rev. Lett.* **85** 2380
[44] Buyers W J L, Morra R M, Armstrong R L, Hogan M J, Gerlach P, and Hirakawa K 1986 *Phys. Rev. Lett.* **56** 371
[45] Tun Z, Buyers W J L, Armstrong R L, Hirakawa K, and Briat B 1990 *Phys. Rev. B* **42** 4677
[46] Ma S, Broholm C, Reich D H, Sternlieb B J, and Erwin R W 1992 *Phys. Rev. Lett.* **69** 3571
[47] Regnault L P, Zaliznyak I, Renard J P, and Vettier C 1994 *Phys. Rev. B* **50** 9174
[48] Haverkort M W 2010 *Phys. Rev. Lett.* **105** 167404
[49] Ren J, Wang Y P, and Fang C 2024 *Phys. Rev. B* **110** 245101
[50] Fishman M, White S, and Stoudenmire E 2022 *SciPost Phys. Codebases* 4